

AN EXPERIMENT REVEALING THE MOTION OF THE EARTH THROUGH A MEDIUM

Michele Zanoni¹

¹I.I.S.S. "F. Gonzaga", Via F.lli Lodrini, 32, 46043 Castiglione delle Stiviere, ITALY. physiszano@gmail.com

The results of a simple experiment are reported. Circuits, like data-loggers, containing FET electronic components reveal a particular signal when working in the tri-state mode (floating pin). Time series recorded by two identical circuits (antennae) at distances of thousands of kilometers show identical daily spectrograms and correlation time delay. In particular the daily correlation time delay curve confirms, over the 99.99 % confidence limit, the motion of the Earth through a medium filled with a field generating the signal fluctuations. Such a field appears homogeneously distributed all around the Earth orbit as proved by the best fit with a simple model providing a flux speed of about 37 ± 4 km/s in the direction of the motion of the Earth in the solar frame system. Some final considerations are formulated by analyzing the power spectrum of the signal apparently different from both a Lorentzian and a Planckian distribution. This seems to exclude that the origin of the signal could be ascribed to respectively Random Telegraph Noise (RTN) and particles obeying the Bose-Einstein statistics.

1 Introduction

In this paper I mainly report the results of an experiment operating from July 23 2022 till July 28 2022, with two identical devices (antennae in this paper) which will be described in section 2. One of the antennae was placed in Tricase in the South of Italy (antenna B) and the other in Guidizzolo in the North of Italy (antenna A). Due to the electronic FET components contained in these two identical detectors, they exhibit fluctuating but correlated output voltages. The linear distance between them is about 880 km (neglecting the curvature of the Earth). The aim of the experiment was to reveal time delays between the two antennae due to the motion of the segment connecting the antennae as regard to an hypothetical flux of the signal supposing it is coming from outside the Earth. This experiment is only the latest version, at last the most robust and persuasive, in the context of a research that the author has been working for several years. Therefore, as a support to the thesis shown in this paper, some of the results of other related experiments, which have been worked out in different versions by the author since October 2005, will be used. From a first experimental stage very similar spectrograms (see example in fig. 1) come out representing the Discrete Stockwell Transform (DST) of the data simultaneously recorded from antennae placed in very distant and different spots.

The use of the DST is supported by the fact that this transform is capable to emphasize variation trend in the evolution of phenomena. The spectrograms shown were realized disposing the DST colored amplitude on a vertical line (blue minimum value, red maximum value) with the frequency growing from the bottom to the top up to 0.1248 Hz and placing the DST lines beside each other moving time from left to right from 0 till 24 hours. An amazing strong similarity appears comparing signals detected by antennae displaced

far away from each other in different directions. Guidizzolo (IT - coordinates 45° 19' N 100° 34' E) where a stable antenna worked since December 2016. Identical antennae were placed in different place, such as La Spezia, Lecce, Torino, Marsala in Italy or even Athens, Sevilla, Lisboa, Tenerife. At a wider distance (NY or Melbourne) this similarity disappears although of signals in the range 20-25 mHz still appear very similar, nevertheless this fact suggests the existence of a correlation length. Actually the results of these experiments were obtained without shielding the devices at all. Evidently amounts of energy and the slow varying evolution in time of the detected events support the motivation for not checking environmental parameter hence, for the same reason, there is no need for sophisticated filtering electronics in order to reproduce the experiment.

As a matter of fact simply by plugging a wire (antenna) in a data-logger analog pin, the voltage output suddenly starts to float between a minimum and a maximum value (up to 5 volts in the Arduino shields used as data-loggers interfaces and connected to a laptop). Choosing a sampling in a range 0.05 – 0.5 s the output voltage starts to fluctuate as soon as the serial monitor in the Arduino sketch is opened. This is the simple device used in the experiment described in this paper. Something to avoid in engineering, or even dangerous for certain circuits, this signal has instead really interesting features in physics as it will be demonstrated in this paper. On the other hand the origin of the tri-state fluctuation is very complicated to analyze and in some way it is related to the mysterious origin of the 1/f noise (for an historical perspective see [1] and reference therein). For example, for small sampling (about 0.02 s) the Arduino tri-state output voltage reveals the typical beat pattern produced by the interference of two frequencies near 50 Hz *. For bigger sampling (0.2 s

*The beat is generated by the interference between the sampling fre-

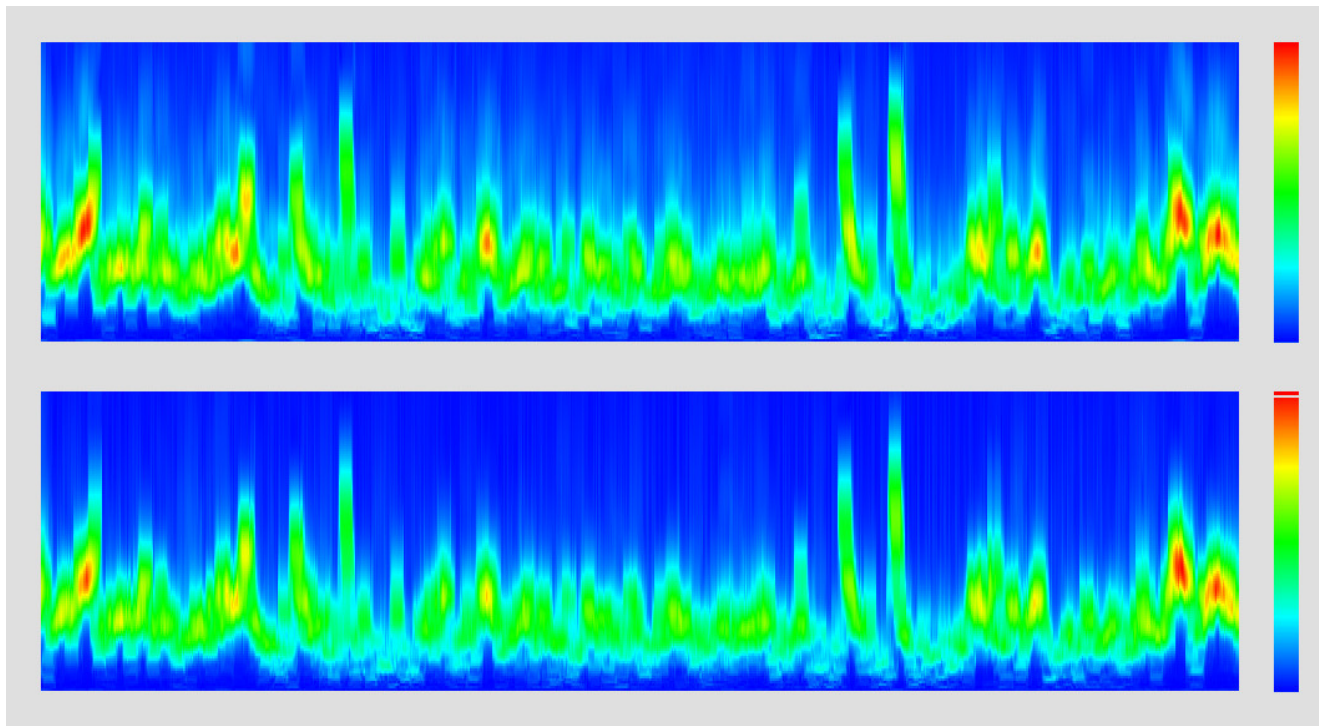


Fig. 1: These spectrograms compare the signal detected in Guidizzolo (above) and Sevilla (below) during 24 hours on Mar 31, 2018. Both the computers were synchronized at CET

as in the present experiment) we can realize that the tri-state fluctuation is evidently produced by the interference of the sampling with the radiation produced by the EU Electricity Network. The very small variation of the beat frequency occurring in a MOSFET component is probably not induced by the Random Telegraph Noise generated inside the Arduino ports [2] as we will see in section 4. The study of the interaction generating the beat interference is fundamental to understand the microscopic transduction of the signal, but this is out of the aim of this work.

2 The Experiment

In the time-voltage diagram in fig. 2 the signals from two different places at the same time (march 31 2018 around 0 hour and 30 minute local time) are plotted. We recognize the common pattern with some little variations of frequency and phase. The related cross-correlation function is plotted in the upper part of figure 2. The signals revealed by the two antennae (in the example in figure 1 one set in Guidizzolo - Italy and the other one in Sevilla – Spain) appear very similar and shifted only by a phase factor. The fluctuation varies very slowly and for this reason the signal is quite simple to detect, record and process with a commercial mobile PC.

quency and a lightly varying frequency related to the radiation produced by the European Electric Network (working at 50 Hz) and perturbing the electronic components.

The device chosen for this experiment consists essentially only of an Arduino DUE (fig.4) shield with 5 cm long, 1 mm diameter aluminum wire plugged in the the A0 analog pin of the shield. Arduino DUE can work as data logger using 12 bit instead of the 10 bit of Arduino UNO.

The analog pins of an Arduino shield are connected in a serial cascade of N MOSFET components where N is the number of the analog pin (12 in the Arduino DUE shield) [3]. In other words a sequence of modules each one represented in the scheme described in figure 4. The main problem in the gathering data with two devices regards the synchronization of the sampling. Choosing a sampling of 0.2 s (as in the present experiment) two Arduino clocks collect differences (retard) of several seconds for the 5-days-long experiment here reported. Such a difference between the clocks of the two Arduino shields are normal but unacceptable in order to measure time delays between two antennae. This problem has been solved in the last version of the experiment (here presented) by using the GPS time provided for a single antenna by the system composed of an Arduino UNO connected to a Neo-6m GPS module. The GPS system provides freely the so called Fix or a 1 second cadence pulsed by a complex system implementing measurement of time with atomic precision [4]. This further improvement guarantees the antennae to remain synchronized during the whole experiment (actually only few data have been pruned with a simple al-

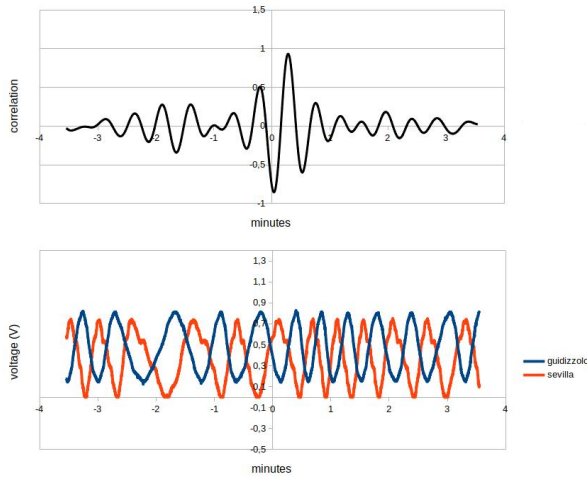


Fig. 2: Bottom: Output voltage. Red for the Sevilla signal (Spain) and blue for the Guidizzolo signal (Italy). Top: Correlation function (black) for the signals above

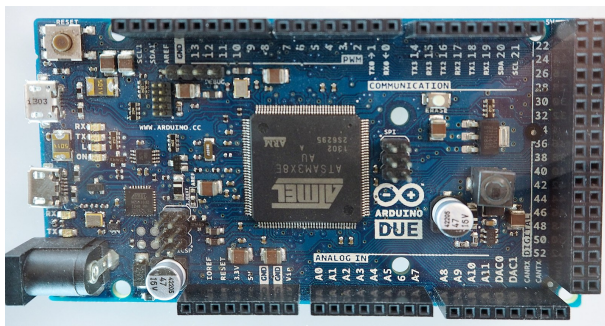


Fig. 3: The Arduino DUE shield

gorithm. The scheme in figure 5 describes the experimental setup with a Linux PC on the right. In order to demonstrate the interaction between a FET component with the perturbation an external circuit it has been used as briefly described in the section 4.

3 Results - Time delay

The time series obtained from the latest experiment performed in July 2022 have been processed with the following method. Unfortunately the sequence of cross-correlation plots rarely show a regular variation of the correlation delays because of fluctuation in phase of the two signals (as proved by the comparison of time series of two antennae placed in the same site).

The way chosen to proceed requires to open a wide mobile temporal window on the cross-correlation graph and averaging time delays of the maxima of the cross-correlation graph from one side and the time delays of minima from the other side. In this way we obtain two time delay time series (plotted respectively as blue and red circles in the graph in fig.

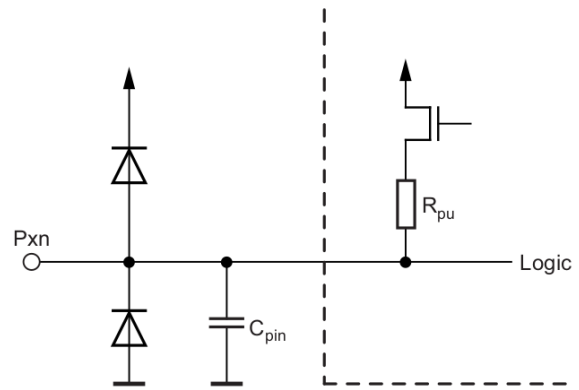


Fig. 4: Scheme of a single Arduino port

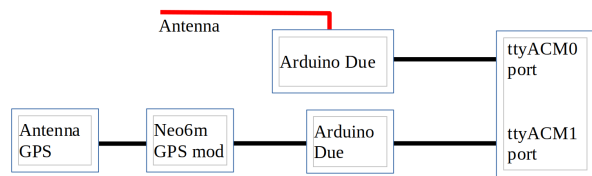


Fig. 5: Scheme of the experimental setup

8). On second stage it was necessary to apply a mobile average in order to smooth both the graphs of the time delays. The temporal window chosen was 360 minutes long (from 3 hours before to 3 hours after a single channel). After dividing the daily 720 files (one file each 2 minutes) in 90 channels and averaging on the 8 data contained in each single channel, we obtain the plot in figure 6.

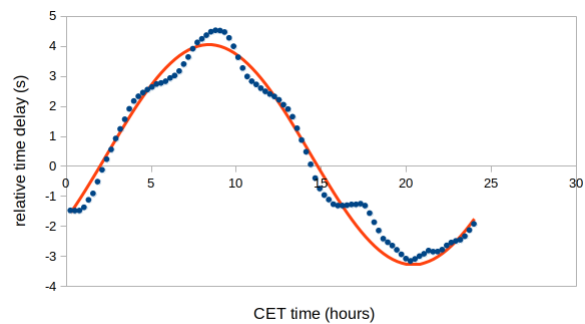


Fig. 6: comparison between the 90 channels mobile average of the experimental data (blue dots) and the model obtained from the best fit (red line)

Because all the time delay intervals are relative amounts or, in other words, any single time delay value differs from the real value for a fixed unknown constant, we can subtract a fixed constant (selected by a best fit algorithm described

below) to all data obtaining the plot in figure 7.

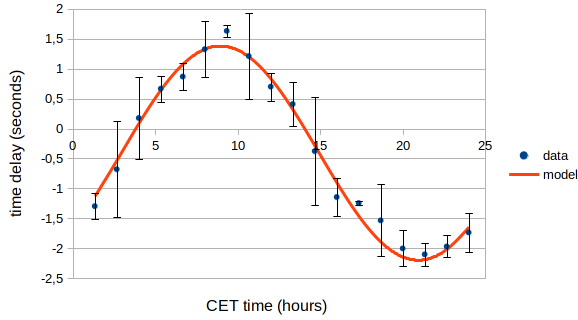


Fig. 7: comparison between the 18 channels experimental data (blue dots) and the model obtained from the best fit (red line)

The red line (time delay function Δ) in both previous plots refer to a model based on the calculation of the scalar product of the flux field \vec{F} and the vector \vec{d} representing the vector distance between the two antennae (in fig. 8 the \vec{F} and \vec{d} vectors are respectively the black one and the purple one). In fact, the best values of the parameters (direction of the incoming signal and its relative velocity) are obtained calculating the minimum χ^2 over a complete diurnal rotation of the Earth and varying the direction of the flux \vec{F} all over the Earth. Fixing the vector $\vec{d} = (-394, 654, 437) \text{ km}$ at $t=0$ and, being θ and ϕ respectively the equatorial coordinates that define the incoming direction of the stream, and defining the generic flux direction $\vec{F} = (\cos(\theta)\cos(\phi), \sin(\theta)\cos(\phi), \sin(\phi))$ then the time delay function Δ , for a rotation starting from $t=0$, is:

$$\Delta = \frac{1}{v} \left((-397\cos(\omega t) - 654\sin(\omega t))\cos(\theta)\cos(\phi) + (-397\sin(\omega t) - 654\cos(\omega t))\sin(\theta)\cos(\phi) + (437\sin(\phi)) \right) \quad (1)$$

Where v is the (relative) speed of the stream (flux) in km/s, ω is the angular speed of the Earth.

Furthermore the experiment was repeated with the same two antennae and connected devices placed in the same place in Guidizzolo in order to demonstrate the reality of the time delay effect. The proposed modus operandi to process the experimental data essentially provides the calculation of the cross-correlation function for a couple of the synchronized data files recorded by the two antennae (file data A from Guidizzolo, file data B from Tricase). Comparing consecutive cross-correlation functions we do not observe the expected regular shifting of the peek of the function, instead a swinging in phase. By averaging the delay of the peeks exceeding a particular probability soil ($|p| > 0.4$ in this work) in a wide temporal window (from three hours before to three

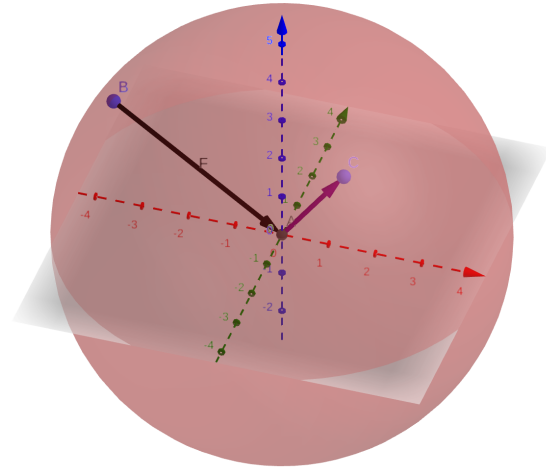


Fig. 8: representation of the vector flux (black) and the vector \vec{d} (purple)

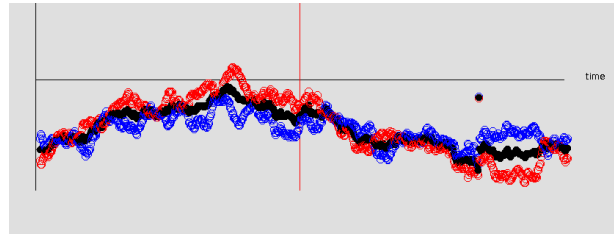


Fig. 9: trend of the delay for maxima (blue circles) and minima (red circles). The black filled circle are the mean values

hours later) we obtain the daily mean distribution of the relative time delay (fig. 9). We finally calculate the direction of the incoming signal with a second Java program making rotate the flux \vec{F} around the Earth and selecting the direction having the minimum χ^2 .

In figure 10 we find a representation of the results of the best fit algorithm for the 90 channel partition. In red we see the higher values of the χ^2 , in blue the lower values. The numerical results obtained are described in tab 1.

Tab. 1 – Tricase – Guidizzolo antennae				
chan	χ^2	θ	ϕ	speed
N	(*)			(km/s)
18	$4,96 \pm 0,29$	$245^\circ \pm 4^\circ$	-42°	37 ± 4
90	$33,7 \pm 1,5$	$245^\circ \pm 4^\circ$	$-33^\circ \pm 14^\circ$	37 ± 4
720	257	$245^\circ \pm 4^\circ$	16.2°	40

(*) the number of degrees of freedom is $N - 4$ in all the cases

The results obtained are very close to the tabulated values defining the direction of the Earth orbital motion in the period

July 23 – 28, 2022 in equatorial coordinates:

$$\theta = 249^\circ \pm 1^\circ$$

$$\phi = -19.5^\circ \pm 0.5^\circ$$

the speed of the incoming signal is very close to the orbital speed of the Earth at that period of time (about 34 km/s). As a final remark we note that, for the 90 channels partition, the values of the χ^2 test provide a probability of more than 99.99% to accept the hypothesis (tab. 1) and a probability less than 0.05% in the case of the two antennae working in the same place (tab. 2).

Tab. 2 – Guidizzolo – Guidizzolo antennae

chan	χ^2
N	(*)
18	26.8
90	143

(*) the number of degrees of freedom is N – 4 in all the cases

4 Results - Power Spectrum

With a third Java program we can obtain the power spectrum of the signal. The plot of the spectral density reveals the predominance of the 1/f noise. Subtracting the 1/f noise the distribution plotted in fig. 11-12 appears. In order to obtain a sufficiently enlarged distribution the sampling was fixed at 1 second. In particular, in the plot the experimental data (blue dots) are compared with the Planck distribution (orange), Landau fitting (green), Lorentzian fitting (brown) and with a mathematical function describing the distribution for high frequency (yellow) very well.

As reported in literature [5], the power spectrum of the experimental data seems not to follow a typical RTN spectrum. In order to demonstrate the external origin of the fluctuation the circuit represented in the scheme in fig. 13 it has been tested.

several sets of data were obtained. By processing these data sets, the power spectrum described in the fig. 12 have been obtained, which confirms and quantifies the power spectrum described in the fig. 11.

5 Conclusion

I tried to convince the reader that a simple experiment performable outside a physics lab independently from environmental conditions provides results revealing the motion of the Earth through an unidentified medium. The results are relevant considering the confidence levels of the measurements and the compatibility with the real reference values for the direction and the relative velocity of the incoming flux. Obviously some aspects of this research must be improved with alternative experiments and enlightening the physical processes involved at a microscopical scale.

A further work will be dedicated to a model that explains the trend of the experimental data plotted in the power spectra (figures 11 and 12) at least for high frequencies (for lower

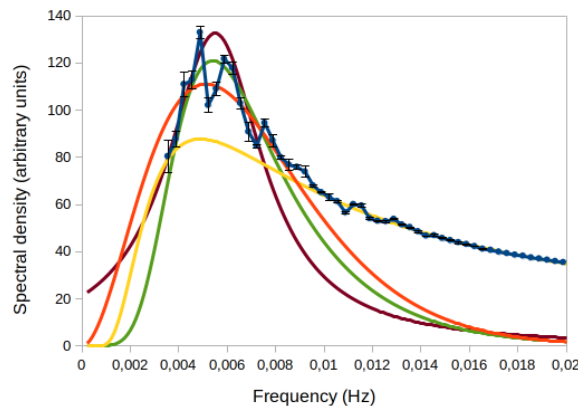


Fig. 10: Spectral density: experimental data (blue dots) compared with the Planck distribution (orange), Landau fitting (green), Lorentzian fitting (brown) and with a mathematical function describing the distribution for high frequency (yellow)

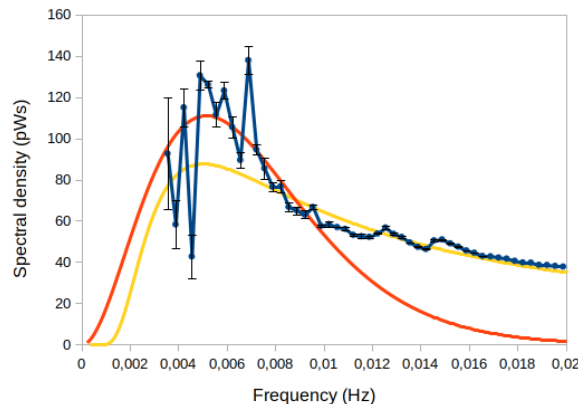


Fig. 11: Spectral density for an experiment performed using the detector described in the scheme in fig. 13

frequencies it was really difficult to separate this spectrum from the 1/f one). Finally, some considerations will be extrapolated about the field causing the revealed effect and the amounts of energy involved in this phenomenon.

Acknowledgements

I wish to thank all the people participating in different ways to this work. A special thank to my best friend Enzo Campion, who died recently and whose contribution was essential.

Submitted on October 9, 2022 / Accepted on Month Day, Year

6 References

References

1. D. M. Fleetwood, Origins of 1/f Noise in Electronic Materials and Devices: A Historical Perspective, Noise in Nanoscale Semiconductor Devices pp 1–31

2. see for example A. Teramoto - Evaluation of Low-Frequency Noise in MOSFETs Used as a Key Component in Semiconductor Memory Devices - *Electronics* 2021, 10(15), 1759; <https://www.mdpi.com/2079-9292/10/15/1759/htm>
3. Atmel-7810-Automotive-Microcontrollers-ATmega328P-Datasheet.pdf, pag. 58 - downloadable at <https://www.microchip.com/en-us/product/atmega328p>
4. see the official site <https://www.gps.gov/systems/gps/>
5. Z. Çelik-Butler - Measurement and Analysis Methods for Random Telegraph Signals – Advanced Experimental Methods For Noise Research in Nanoscale Electronic Devices, pp 219–226 <https://link.springer.com/chapter/10.1007/1-4020-2170-4-25>



Fig. 12: This work is licensed under the Creative Commons Attribution 4.0 International License. To view a copy of this license, visit <http://creativecommons.org/licenses/by/4.0/> or send a letter to Creative Commons, PO Box 1866, Mountain View, CA 94042, USA.